International Journal of Thin Films Science and Technology

http://dx.doi.org/10/12785/ijtfst/020207

# Impact of dilution gases on structure, properties and growth of hydrogenated nanocrystalline silicon (nc-Si:H) prepared by HW-CVD method

**Nabeel A. Bakr[1], Tahseen H. Mubarak[1], Nadir F. Habubi[2]**

[1]*Department Of Physics, College of Science, University of Dyiala, Diyala, Iraq*
[2]*Department of Physics, College of Education, Al-Mustansiriyah University, Baghdad, Iraq*

*Email: nabeelalibakr@yahoo.com*

Received: 11 July. 2012, Revised: 2 Feb. 2013; Accepted: 10 Mar. 2013
Published online: 1 May 2013

**Abstract:** In this work we present a detailed structural, optical and electrical characterization of hydrogenated nanocrystalline silicon (nc-Si:H) thin films grown by hot wire chemical vapor deposition (HW-CVD) as a function of hydrogen ($H_2$), argon (Ar) and helium (He) dilution of silane. A variety of analysis techniques such as Raman spectroscopy (RS), x-ray diffraction (XRD), Fourier transform infrared (FTIR) spectroscopy, UV-Visible spectroscopy and conductivity measurements were used to characterize the grown films. We observed that these properties are greatly influenced by dilution of silane with $H_2$, Ar and He. Characterization of these films by Raman spectroscopy and low angle x-ray diffraction revealed that the increase in $H_2$ and Ar dilution of silane endorses the growth of crystallinity in the films whereas increase in He dilution of silane deteriorates the film properties. An attempt has been made to explain the fundamental differences in nanocrystallization growth mechanism by addition of $H_2$, Ar and He in silane.

**Keywords:** HW-CVD, nc-Si:H, Hydrogen Dilution, Argon dilution, Helium dilution

## 1. Introduction

During the last few years, hydrogenated nanocrystalline silicon (nc-Si:H) material have attracted great attention due to their different potential applications in photovoltaics, thin film transistors and optoelectronics devices [1]. In the field of single or multijunction solar cells, nc-Si:H thin films have shown an remarkable enhancement in solar cell efficiencies and in their stability [2]. Several deposition techniques have been established to prepare nc-Si:H thin films, including plasma enhanced chemical vapor deposition (PE-CVD) [3] and its variant very high frequency glow discharge (VHF-GD) [4], electron cyclotron resonance-CVD (ECR-CVD) [5] and radio-frequency (RF) magnetron sputtering, among which PE-CVD appears to be a promising deposition method for large-area thin film technology and has been employed for industrial applications [6]. However, due to certain material and processing limitations, other deposition techniques have been developed and examined. Among these is the hot wire chemical vapor deposition (HW-CVD) technique, first developed by Weisman [7] and then later refined by Matsumura [8]. The technique has been employed successfully for the synthesis of a-Si:H [9], μc-Si:H [10], nc-Si:H [11], a-SiGe:H [12], μc-SiC and μc-GeC films for solar cell applications [13] because it is

@ 2013 NSP
Natural Sciences Publishing Cor.

capable of improving film stability [14] and of achieving higher deposition rates [15]. The technique is attractive in many ways and the most important advantages are: (i) Plasma-free deposition so that the damaging of the deposited film and powder formation during the deposition can be avoided (ii) It is an easily scalable method. (iii) Deposited films have less stress than those made by conventional PE-CVD method [16] (iv) Substrates can easily be handled as they do not have a role in the decomposition process. (v) High flux of atomic H generated in HW-CVD helps to remove highly strained bonds and to decrease structural disorder etc. Moreover, the technique involves very few deposition parameters which can easily be optimized, and the film growth processes involve simple radicals which are primarily atoms (e.g. Si, H) released from the hot surface [17].

In HW-CVD, many authors have reported that the amorphous-to-nanocrystalline transition occurs mainly due to hydrogen dilution of silane [18-22]. To best of our knowledge, only few reports exist in the literature about using noble/inert gas dilution of silane for the synthesis of nc-Si:H films by the HW-CVD method[23]. With this motivation we initiated the detailed study of synthesis and characterization of nc-Si:H films with hydrogen ($H_2$), argon (Ar) and helium (He) dilution of silane ($SiH_4$) (defined as $R_{Diluent} = \frac{F_{Diluent}}{F_{Diluent} + F_{SiH4}}$) by using HW-CVD method. Here, $F_{Diluent}$ and $FSiH_4$ are the dilution gas flow rate and silane gas flow rate respectively. In this paper, we present the preliminary results of investigation of structural, optical and electrical properties of nc-Si:H films deposited by HW-CVD method as a function of $H_2$, Ar and He dilution of silane. It has been observed that these properties are greatly affected by $H_2$, Ar and He dilution of silane.

## 2. Experimental

Intrinsic hydrogenated nanocrystalline silicon (nc-Si:H) thin films were deposited simultaneously on corning #7059 glass and c-Si wafers in a HW-CVD system, details of which have been described elsewhere [24]. Three sets of films were prepared by using a mixture of pure silane ($SiH_4$) (Matheson Semiconductor Grade) and $H_2$, Ar and He gases separately. In order to study the influence of the different gases dilution of silane on structural, optical and electrical properties of the films, the diluent gas flow rate was kept constant (30 sccm) and the silane flow rate was varied from 1 to 20 sccm so that $R_{Diluent}$ is varied between 60 and 97 %. The temperature of the filament was maintained at 1900 ± 25 $^0$C. The substrate temperature was held constant (450 $^0$C) during the deposition using a thermocouple and temperature controller with an error of ± 5 $^0$C. The deposition parameters are listed in Table 1.

**Table 1:** Deposition parameters for preparation of nc-Si:H thin films Parameter.

| | Set-I | Set-II | Set-III |
|---|---|---|---|
| Filament temperature ($T_f$) | 1900 $^o$C | 1900 $^o$C | 1900 $^o$C |
| Substrate to filament distance ($d_{s-f}$) | 2.75 cm | 2.75 cm | 2.75cm |
| Silane flow rate ($F_{SiH4}$) | 1-20 sccm | 1-20 sccm | 1-20 sccm |
| Hydrogen flow rate ($F_{H2}$) | 30 sccm | ----- | ----- |

@ 2013 NSP
Natural Sciences Publishing Cor.

| | | | |
|---|---|---|---|
| Argon flow rate ($F_{Ar}$) | ----- | 30 sccm | ----- |
| Helium flow rate ($F_{He}$) | ----- | ----- | 30 sccm |
| Substrate Temperature ($T_{sub}$) | 450 $^{o}$C | 450 $^{o}$C | 450 $^{o}$C |
| Deposition pressure (P) | 50 mTorr | 50 mTorr | 50 mTorr |
| Time of deposition | 10-60 min | 10-60 min | 10-60 min |

The dark conductivity ($\sigma_{dark}$) and photoconductivity ($\sigma_{photo}$) were measured with a coplanar Al electrode. Fourier transform infrared (FTIR) spectra of the films were recorded by using FTIR spectrophotometer (Shimadzu, Japan). Bonded hydrogen content ($C_H$) was calculated from wagging mode of IR absorption peak using the method given by the Brodsky et al. [25]. The optical band gap was estimated using the procedure followed by *Tauc* [26]. Raman spectra were recorded with micro-Raman spectroscopy (Jobin Yvon Horibra LABRAM-HR. The spectrometer has backscattering geometry for detection of Raman spectrum with the resolution of 1 $cm^{-1}$. The excitation source was 632.8 nm line of He-Ne laser. The power of the Raman laser was kept less than 5 mW to avoid laser induced crystallization on the films. The Raman spectra were deconvoluted in the range 400-540 cm-1 using *Levenberg-Marquardt* method [27]. The crystalline fraction ($X_{Raman}$) was then deduced using the method proposed by Kaneko et al. [28]. The crystallite size ($d_{Raman}$) was calculated from $d_{Raman} = 2\pi\sqrt{\left(\frac{B}{\Delta\omega}\right)}$, where $\Delta\omega$ is the peak shift for the hydrogenated nanocrystalline silicon (nc-Si:H) compared to the crystalline silicon (c-Si), and B = 2.0 $nm^2$ $cm^{-1}$ [29]. Low angle x-ray diffraction spectra were obtained by x-ray diffractometer (Bruker D8 Advance, Germany) using Cu $K_\alpha$ line ($\lambda$ = 1.54056 Å). The spectra were taken at a grazing angle of $1^0$. The average crystallite size was estimated using the classical *Scherrer's* formula, $d_{x-ray} = \frac{0.9\,\lambda}{B\cos\theta_B}$ [30].

The thickness of films was determined by Talystep profilometer (Taylor-Hobson Rank).

## 3. Results and Discussion

### *3.1 Variation in Deposition Rate*

Variation of deposition rate ($r_d$) plotted as a function of hydrogen ($H_2$), argon (Ar) and helium (He) dilution of silane ($R_H$, $R_{Ar}$ and $R_{He}$) is shown in figure 1. As seen from the figure, for all dilutions of silane ($R_H$, $R_{Ar}$ and $R_{He}$) the deposition rate decreases with increase in dilution of silane by the diluent gas. Decrease in deposition rate can be attributed to decrease in $SiH_4$ density in the gas mixture. With increase in dilution of silane with diluent gas, the concentration of precursors that produces Si:H film decreases.

Consequently, the deposition rate decreases with increasing the dilution of silane by the diluent gas. Furthermore, the deposition of film involves two simultaneous processes; the first is the growth of film forming radicals and the second is the etching of deposited portion. Therefore, the deposition rate is determined from the competition between both the deposition and the etching processes. The low deposition rate observed for hydrogen dilution of silane is undoubtedly related to a more efficient etching

@ 2013 NSP
Natural Sciences Publishing Cor.

process in the deposition-etching competition compared to argon and helium diluted films. The etching effect of hydrogen atoms has been experimentally verified [31]. The higher deposition rate observed for argon and helium diluted films compared to that of hydrogen diluted films under the same deposition conditions can be correlated to the non-etching properties of argon and helium [32].

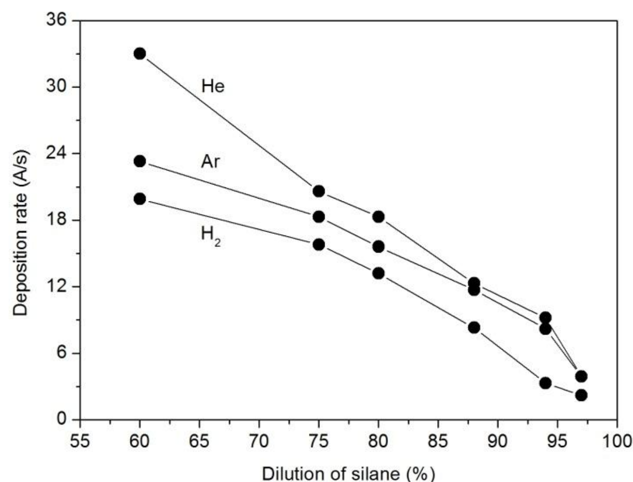


**Figure 1:** Variation of deposition rate as a function of dilution of silane by $H_2$, Ar and He gases.

### *3.2 Micro-Raman Spectroscopic Analysis*

Figure 2 shows Raman spectra of films deposited at hydrogen ($H_2$), argon (Ar) and helium (He) dilution of silane ($R_H$, $R_{Ar}$ and $R_{He}$). Each spectrum shown in figure 2 was deconvoluted into two Gaussian peaks and one Lorentzian peak with a quadratic base line using *Levenberg-Marquardt* method to calculate volume fraction of crystallites ($X_{Raman}$) and crystallite size ($d_{Raman}$) in the film. The estimated $X_{Raman}$ and $d_{Raman}$ in the film are also indicated in each figure. As seen from figure 2(a), the film deposited at $R_H$ = 60 % shows a broad rounded peak centered around 480 $cm^{-1}$, which is characteristic of a-Si:H. The film deposited at $R_H$ = 80 % shows the onset of nanocrystallization. The Raman spectrum for this film shows a combination of two TO phonon peaks, one centered around 480 $cm^{-1}$ and the second centered at 501 $cm^{-1}$, the later peak originates from the nanocrystalline phase [33]. This clearly indicates the amorphous-to-nanocrystalline transition. The film deposited at $R_H$ = 80 % shows $X_{Raman}$ ~ 30.3 % and $d_{Raman}$ < 2 nm. By increasing the $R_H$ to 88 %, $X_{Raman}$ and $d_{Raman}$ both increases, which inferred from the non-appearance of amorphous phase and shifting of TO phonon peak to the higher wave number 520 $cm^{-1}$ [34]. Thus, the film deposited at $R_H$ = 97 % shows $X_{Raman}$ ~ 77.6 % and $d_{Raman}$ ~ 20.9 nm. The amorphous-to-nanocrystalline transition and increase in volume fraction of crystallite and its size with increase in $R_H$ in HW-CVD have been reported by many authors [18-22]. However, it is interesting to note that in the present case we have observed amorphous-to-nanocrystalline transition comparatively at low $R_H$. Thus, high hydrogen dilution of silane is not necessary to obtain nc-Si:H films by HW-CVD technique. In HWCVD, every silane molecule upon dissociation yields one Si atom and four H atoms. Also, the hot filament is a very effective source of atomic H [35, 36]. The filament temperature (1900 $^0$C) in HW-CVD decomposes all hydrogen molecules into reactive H atoms. Thus, the density of atomic H in the deposition chamber increases with increase in hydrogen dilution of silane. This increases the etching of Si atoms from disordered and strained bonding sites and giving a nanocrystalline network [37, 38]. As a

result, amorphous-to-nanocrystalline take place with increase in hydrogen dilution of silane. Now let us see the Raman spectra of nc-Si:H films deposited at Ar dilution ($R_{Ar}$) and helium dilution of silane($R_{He}$). As seen from figure 2 (b), film deposited at $R_{Ar}$ = 60 % shows a broad shoulder centred near 480 $cm^{-1}$, which is characteristic of a-Si:H where as the film deposited at $R_{Ar}$ = 80 % shows the onset of nanocrystallization. The Raman spectrum for this film shows a combination of two peaks, one centred ~ 480 $cm^{-1}$ and the second centred ~ 505 $cm^{-1}$ originating from the contribution of small Si nanocrystals. This clearly indicates an amorphous-to-nanocrystalline transition in the film with increase in $R_{Ar}$. For this film, $X_{Raman}$ is ~ 29.2 % and $d_{Raman}$ is ~ 2.0 nm. With further increase in $R_{Ar}$, the TO phonon peak is shifted further towards the higher wave number whereas its intensity and sharpness are reduced indicating increase in $d_{Raman}$ and $X_{Raman}$ in the films. Thus, for the film deposited at $R_{Ar}$ = 97 %, the Raman spectrum shows nanocrystalline phase with the TO phonon peak centered at 519 $cm^{-1}$ and an amorphous content in it. For this film, $X_{Raman}$ is ~ 40.1 % and $d_{Raman}$ is ~ 8.3 nm. Thus, it is concluded that in HW-CVD, similar to increase in hydrogen dilution, an increase in argon dilution of silane an amorphous-to-nanocrystalline occur and volume fraction of crystallites and its size increases. Figure 2 (c) shows Raman spectra of nc-Si:H films deposited at various helium dilution of silane ($R_{He}$). As seen from the figure, the film deposited at $R_{He}$ = 97 %, Raman spectrum shows a broad shoulder centred ~ 480 $cm^{-1}$, which is characteristic of a-Si:H and other centred between 500-506 $cm^{-1}$ corresponding to crystalline phase present in the material. For this film $X_{Raman}$ is 52 % and $d_{Raman}$ is 2.4 nm. With increase in $R_{He}$, $X_{Raman}$ in the films decreases while $d_{Raman}$ remains in the range of 2.4-2.1 nm for the entire range of $R_{He}$ studied. The abrupt drop in the crystalline volume fraction from 52 % for the film deposited at $R_{He}$ = 60 % to 18 % for the film deposited at $R_{He}$ = 75 % indicates adverse/deteriorating effect of helium on growth of crystallinity in nc-Si:H prepared by HW-CVD. It is reported that the metastable state of Ar and He atoms (Ar* and He*) and ions ($Ar^+$ and $He^+$) [39-41] plays a vital role in promotion of nanocrystallization in conventional PE-CVD process.

However, in HW-CVD, the hot filament cannot efficiently ionize argon or helium due to their high ionization energy (15.8 eV and 24 eV respectively). Hence, formation of metastable Ar*/He* and $Ar^+/He^+$ that promotes the structural ordering and nanocrystallization is negligible. We think that in HW-CVD method, Ar and He atoms can achieve thermal energy from the heater and electrons which are emitted by hot tungsten (W) filament [42]. With increasing argon dilution, the density of thermal Ar in the vicinity of growth zone increases. The Gibb's free energy required for the formation of nano-crystallites in the amorphous matrix [43] is supplied by the thermal Ar. The energy transferred by the thermal Ar to the growth zone is utilized in breaking weak Si-Si bonds. The dangling bonds resulting from the breaking of weak Si-Si bonds form strong bonds with Si or are terminated by H. This may help in structural reorientation leading to the formation of a more compact network and hence nanocrystallization. However, in case of helium dilution adequate Gibb's free energy is not available in the growth zone due to low mass of He (Helium is ten times lighter than Argon [44]). This results in inefficient thermal energy transfer to the growing surface which attenuates the process of crystallinity in the film. As a result, the volume fraction of crystallites in the films decreases with increase in helium dilution of silane.

@ 2013 NSP
Natural Sciences Publishing Cor.

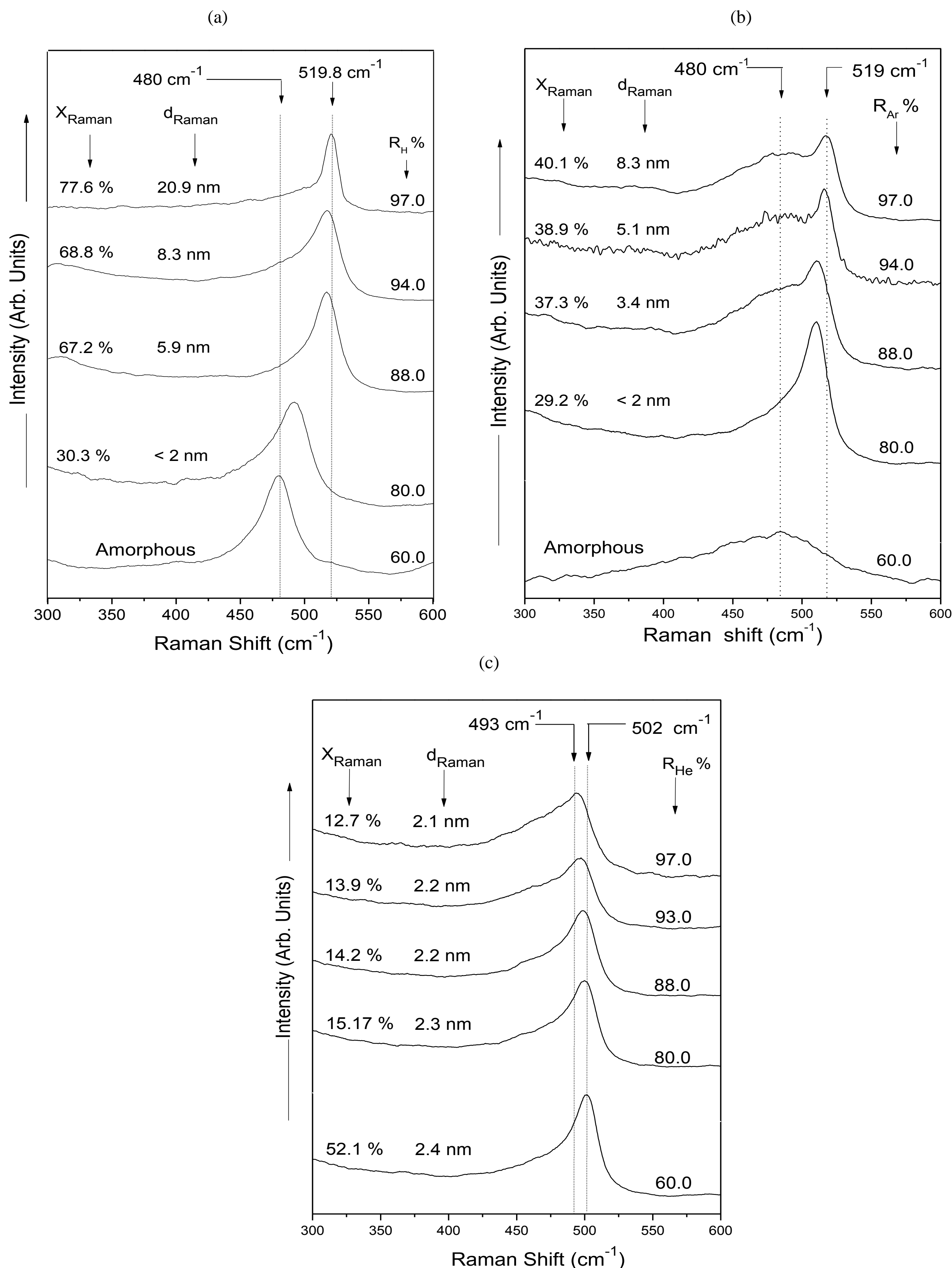


**Figure 2:** Raman spectra of films deposited at different dilution of silane using different diluents (a) Hydrogen dilution of silane (b) Argon dilution of silane and (c) Helium dilution of silane.

@ 2013 NSP
Natural Sciences Publishing Cor.

### 3.3 Low Angle X-Ray Analysis

The x-ray diffraction patterns of nc-Si:H films deposited at hydrogen ($H_2$), argon (Ar) and helium (He) dilution of silane ($R_H$, $R_{Ar}$ and $R_{He}$) is shown in figure 3. As seen from figure 3 (a), the film deposited at $R_H$ = 75 % shows a broad shoulder centered at 2θ ~ 25° indicating that the film is amorphous. The film deposited at $R_H$ = 80 % shows the onset of nanocrystallization with a peak at 2θ ~ 28.2° and less intense peaks at 2θ ~ 47° and ~ 56° corresponding to (111), (220) and (311) crystal orientations.

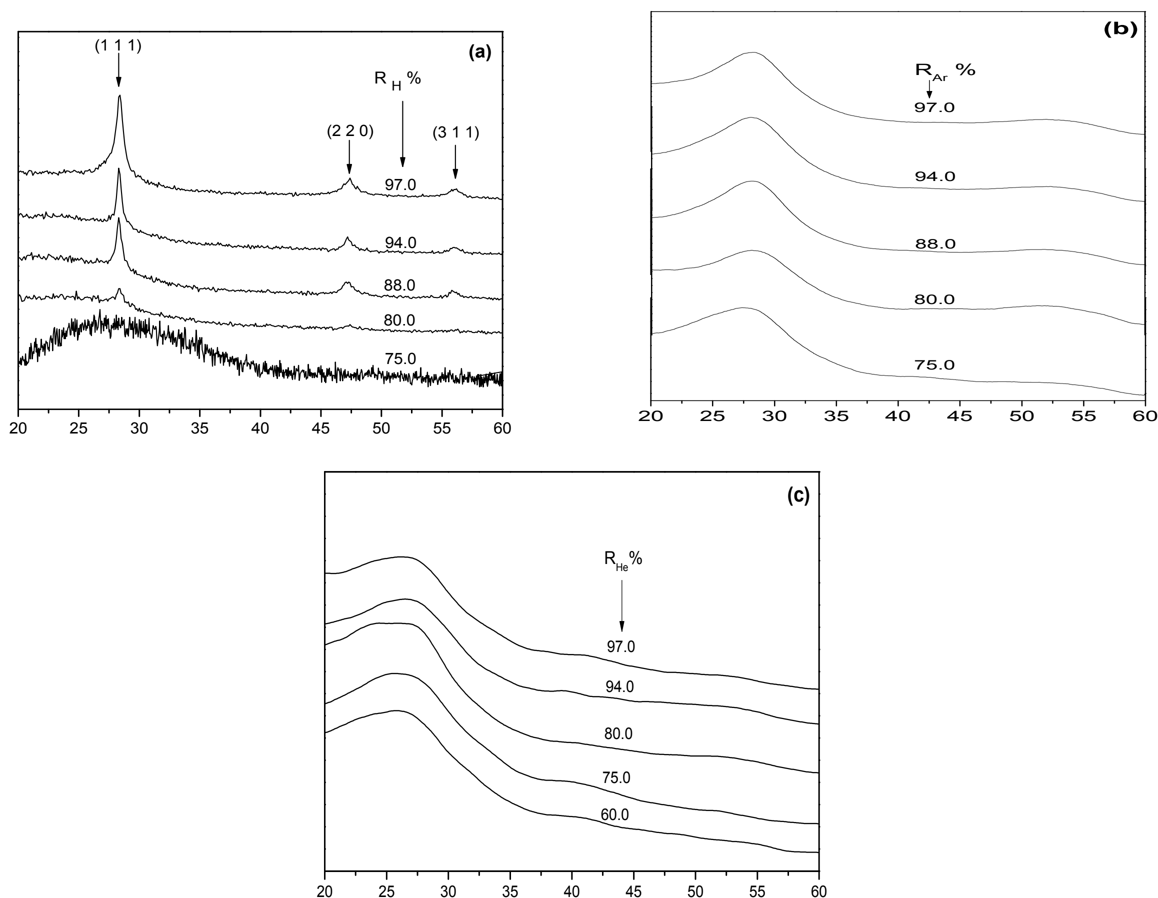


**Figure 3:** X-ray patterns of films deposited at different dilution of silane using different diluent **(a)** Hydrogen dilution of silane **(b)** Argon dilution of silane and **(c)** Helium dilution of silane.

These results indicate that the crystallites in the films have preferential orientation in (111) directions. It is also observed that with increase in $R_H$ the intensity of (111) diffraction peak enhances whereas its line width get reduced. These results indicate that the crystallite size ($d_{x\text{-ray}}$) and its volume fraction ($X_{x\text{-ray}}$) increase with increasing hydrogen dilution of silane. Figure 3(b) shows the x-ray spectra of nc-Si:H films deposited at different Ar dilution of silane ($R_{Ar}$). Similar to figure 2(a), a broad band centered at 2θ = $25^0$ has been observed for the film deposited at $R_{Ar}$ = 75 % indicating amorphous nature of the film. The only

@ 2013 NSP
Natural Sciences Publishing Cor.

feature observed for all films is a broad shoulder occurring at $2\theta = 28.3^0$ corresponding to (111) crystal orientation. Furthermore, a broadening of (111) diffraction peak has been observed with increasing $R_{Ar}$ suggesting increase in $d_{x\text{-ray}}$ of Si nanocrystals in films. The other noticeable change observed in the diffraction spectra is the enhancement of (111) diffraction peak intensity which can be attributed to increase in $X_{x\text{-ray}}$. These results are consistent with Raman analysis. Thus, with increase in argon dilution of silane the volume fraction of crystallites as well as the crystallite size in the film increases. The impact of helium dilution of silane ($R_{He}$) on nc-Si:H films is shown in figure 3(c). The only feature observed for all films is a broad peak occurring at $2\theta = 27.9^0$ corresponding to (111) crystal orientation and less intense peaks occur at $2\theta \sim 41^0$ and $2\theta \sim 53.4^0$ corresponding to (200) and (311) crystal orientations. The dominant peak is (111). The perceptible change observed in the diffraction spectra are the slight broadening and reduction of intensity of (111) diffraction peak indicating decrease in $d_{x\text{-ray}}$ of Si nanocrystals and decrease in $X_{x\text{-ray}}$ with increase in $R_{He}$. These results are consistent with the Raman results and provide further strong support to adverse effect of He on growth of crystallinity in nc-Si:H prepared by HW-CVD.

### *3.4 Variation in Hydrogen Content and Microstructure Parameter*

To reveal the hydrogen bonding configuration and to estimate the total hydrogen content in the film and microstructure parameter, FTIR spectroscopy was used. It was found that the hydrogen content ($C_H$) in Si:H materials calculated from different methods is quite different. However, it has been reported that the integrated intensity of the peak at 630 $cm^{-1}$ is the best measure of hydrogen content and other bands are less reliable [45]. Whatever may be the nature of the hydrogen bonding configuration; SiH, Si-$H_2$, (Si-$H_2$)$_n$, $SiH_3$ etc., all types of the vibrational modes will contribute to the 630 $cm^{-1}$ absorption band [46].

Thus, the hydrogen content has been estimated by using integrated intensity of the peak at 630 $cm^{-1}$ by taking the oscillator strength value determined by *Itoh et al.* [47]. The microstructure parameter (R*) is determined by using $R^* = I_{2100}/(I_{2100}+I_{2000})$, where $I_{2000}$ and $I_{2100}$ are the integrated absorption intensities at 2000 $cm^{-1}$ and 2100 $cm^{-1}$ respectively. Figure 4 shows the variation of hydrogen content ($C_H$) and microstructure parameter (R*) as a function of hydrogen ($H_2$), argon (Ar) and helium (He) dilution of silane ($R_H$, $R_{Ar}$ and $R_{He}$). As seen from figure 4(a) and (b), the $C_H$ in the hydrogen and argon diluted films increases with increase in $R_H$ and $R_{Ar}$. Simultaneously, the R* shows decreasing trend with increase in $R_H$ and $R_{Ar}$.. It is well known that in nc-Si:H films, majority of H is bonded to the surface of the nanocrystallites [48]. As probed by Raman analysis and x-ray diffraction analysis, increase in $R_H$ and $R_{Ar}$ increases the density of nanocrystallite grains in the film due to increase in volume fraction of crystallites. This increases the total surface area of grains which act as reservoirs of H in the material [49]. Thus, increase in hydrogen content with increase in hydrogen and argon dilution of silane can be attributed to increase in increase in volume fraction of crystallites (or decrease in amorphous fraction) in the films. The decreasing trend of R* against $R_H$ and $R_{Ar}$ indicates the enhancement of structural order and homogeneity of the deposited films with increasing $R_H$ and $R_{Ar}$. Figure 4(c) shows the estimated hydrogen content ($C_H$) and microstructure parameter (R*) in nc-Si:H films as a function of helium dilution of silane ($R_{He}$). As seen from the figure, $C_H$ in the helium diluted films decreases with increase in $R_{He}$ while the R* shows increasing trend with increase in $R_{He}$. The increase in R* with increase in $R_{He}$ indicates the deterioration of the film quality with increasing $R_{He}$. These results are in agreement with the results obtained from Raman spectroscopy and x-ray diffraction analysis.

@ 2013 NSP
Natural Sciences Publishing Cor.

### *3.5 Optical Properties*

Variation of band gap ($E_g$) and Urbach energy ($E_{Ur}$) as a function of hydrogen ($H_2$), argon (Ar) and helium (He) dilution of silane ($R_H$, $R_{Ar}$ and $R_{He}$) are shown in figure 5. As seen from figure 5(a), the band gap for the films deposited at various hydrogen and argon dilutions decreases with increase in $R_H$ and $R_{Ar}$. Conversely, for $R_{He}$ it shows growing trend. It is generally accepted that the band gap is dependent on the hydrogen content and it increases with increasing hydrogen content in the films [50]. However, in the present investigation, the hydrogen content in the hydrogen and argon diluted films decreases with increasing hydrogen and argon dilutions of silane (see figure 4a and 4b) whereas for helium diluted films it decreases with increasing helium dilution of silane (see figure 4c). Thus, only the number of Si-H bonds cannot account for the band gap in nc-Si:H films. In addition, there exist several ambiguities about the band gap of nc-Si:H films because the material contains both phases, amorphous and crystalline and their properties vary with the volume fraction of these phases. For the optical band gap estimation, *Tauc's* [51] and Cody's [52] methods are generally employed. The band gap of a-Si:H is between 1.6 and 1.8 eV depending on the process parameters whereas that of c-Si is 1.1 eV.

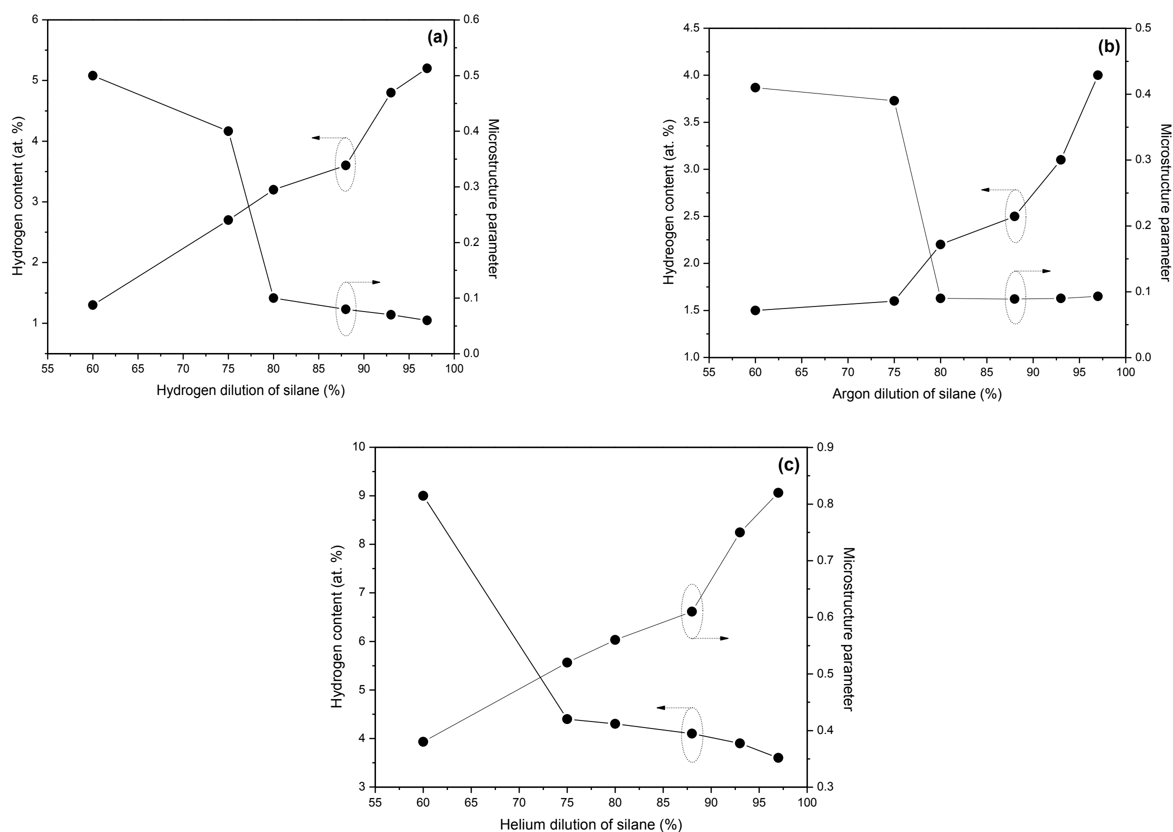


**Figure 4:** Variation of hydrogen content ($C_H$) and microstructure parameter (R*) as a function of dilution of silane using different diluents for the nc-Si:H deposited thin films by HW-CVD.

Accordingly, in the case of a mixed phase of crystalline and amorphous, i. e. nanocrystalline phase, the band gap should lie between values of a-Si:H and c-Si. *Rotaru* et al. [53] have observed a relation

@ 2013 NSP
Natural Sciences Publishing Cor.

between band gap and the content of amorphous silicon using both *Cody's* and *Tauc's* models. They found that the band gap increases with increasing the amorphous content (in the range of 30-100 %) in the film. Thus, we believe that the decrease in band gap with increasing hydrogen and argon dilution of silane may be due to the increase in volume fraction of crystallites (or decrease in amorphous content) in the film, as revealed by the Raman spectroscopic and low angle x-ray diffraction analysis. Figure 5(b) shows the variation of Urbach energy ($E_{Ur}$) as a function of dilution of silane for different diluents. It can be seen from the figure that for $H_2$ and Ar diluted films, the Urbach energy decreases with increasing the dilution of silane and it has value less than 100 meV for the films deposited at higher dilution of silane indicating device quality films [54]. These results are in agreement with the results obtained from FTIR analysis which indicate that $R^*$ is less than 0.1 for the films grown at high dilution of silane (see figure 5a and 5b).

Thus, we conclude that the nc-Si:H films deposited at high hydrogen/argon dilution of silane are compact with less band tails which is characteristic of good quality materials. However, for the He diluted films, the Urbach energy ($E_{Ur}$) of the deposited films increases from 138 to 318 meV as $R_{He}$ increases from 60 % to 97 %. This indicates that the properties of the deposited films degrade with increasing the helium dilution of silane in HW-CVD. This conclusion is well supported by the increasing trend of the microstructure parameter against the helium dilution of silane as indicated in figure 5c.

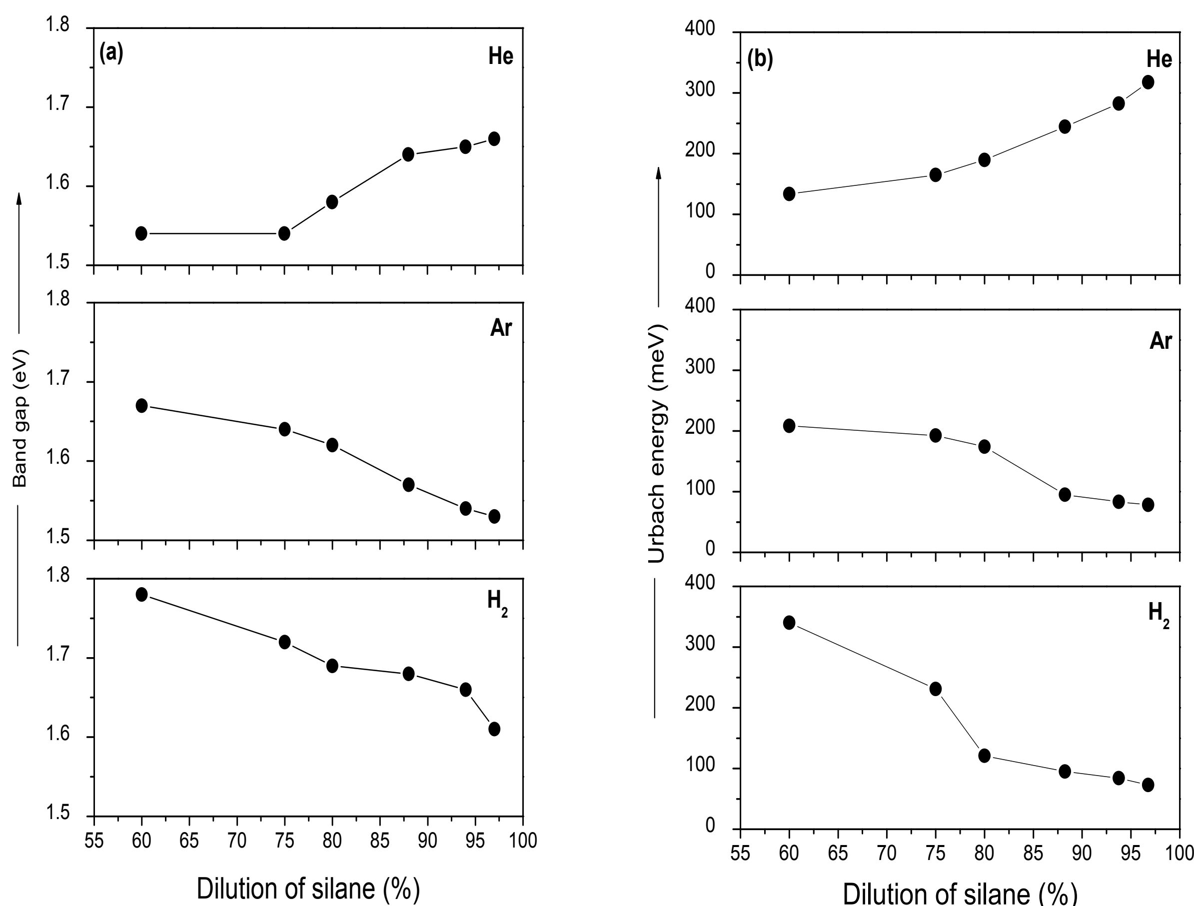


**Figure 5:** Variation of band gap and Urbach energy as a function of dilution of silane using different diluents for the nc-Si:H deposited thin films by HW-CVD.

@ 2013 NSP
Natural Sciences Publishing Cor.

### *3.6 Electrical Properties*

The effect of dilution of silane on dark conductivity ($\sigma_{Dark}$) and photoconductivity ($\sigma_{Photo}$) of nc-Si:H films deposited by HW-CVD using different diluents is shown in figure 6. As seen from figure 6(a) for the hydrogen diluted films, $\sigma_{Dark}$ increases from ~ 4.7x10$^{-10}$ S/cm to ~ 4.2x10$^{-9}$ S/cm and $\sigma_{Photo}$ increases from ~ 7.4x10$^{-5}$ S/cm to ~ 1.54x10$^{-4}$ S/cm when $R_H$ increases from 60 % to 70 %. As a result the photosensitivity ($\sigma_{Photo}$ /$\sigma_{Dark}$) decreases from 1.55x10$^{5}$ for $R_H$ = 97 % to 3.5x10$^{4}$ for the film deposited at $R_H$ = 60 %. For argon diluted films indicated in figure 7(b), $\sigma_{Dark}$ increases by order of 2 (from ~ 10$^{-10}$ S/cm to ~ 10$^{-8}$ S/cm) when argon dilution of silane increases from 60 % to 97 %, whereas the $\sigma_{Photo}$ remains in the range of 10$^{-6}$-10$^{-5}$ S/cm for the entire range of argon dilution of silane studied. As a result, the photosensitivity ($\sigma_{Photo}$ /$\sigma_{Dark}$) decreases from 10$^{5}$ to 10$^{2}$ when argon dilution of silane increases from 60 % to 97 %. This indicates that the films deposited with increasing hydrogen and argon dilution of silane get structurally modified. We attribute the drastic reduction in the photosensitivity to the increase in crystalline volume fraction and crystallite size because the nc-Si:H films prepared by different methods show high dark conductivity and negligible photo-response depending upon the crystallite size and its volume fraction [55]. This inference is further strengthened by the observed variation in deposition rate for hydrogen and argon dilution of silane (see figure 1) because lower deposition rate is more conducive to the formation of crystallinity in the film structure [56]. The effect of helium dilution of silane ($R_{He}$) on dark conductivity ($\sigma_{Dark}$) and photoconductivity ($\sigma_{Photo}$) of nc-Si:H films is shown in figure 6(c).

As seen from the figure, $\sigma_{Dark}$ was found in the range 10$^{-7}$-10$^{-8}$ S/cm and $\sigma_{Photo}$ was in the range 10$^{-4}$-10$^{-6}$ with increase in He dilution of silane increase from 60 % to 97 %. As a result, photosensitivity ($\sigma_{Photo}$ /$\sigma_{Dark}$) increases from 36 to 2.8x10$^{3}$ to when He dilution of silane increases from 60 % to 97 %. We attribute enhancement in the photosensitivity is due to increase in amorphous fraction in the film with increase in He dilution of silane. This inference is further strengthened from Raman spectroscopic results.

## 4. Conclusions

Effect of hydrogen, argon and helium dilution of silane on structural, optical and electrical properties of nc-Si:H films deposited by HW-CVD has been studied in detail. Raman and low angle x-ray diffraction spectroscopic study revealed that with increase in hydrogen and argon dilution of silane the crystallinity as well as crystallite size in the films increases. However, with increase in helium dilution of silane both, the crystallinity and crystallite size in the films decreases. The microstructure parameter decreases with increase in hydrogen and argon dilution of silane whereas it increases with increase in helium dilution indicating that with increase in hydrogen and argon dilution of silane the quality of films improves whereas helium dilution of silane deteriorate the films quality. Measurement of band gap show that it is independent of hydrogen content in the film but it increases with increase in volume fraction of crystallites due to increase in hydrogen and argon dilution of silane and decreases with increase in helium dilution of silane due to reduction of volume fraction of crystallites in the films. The Urbach energy values for nc-Si:H films deposited at high hydrogen/argon dilution of silane are compact with less band tails which is characteristic of good quality materials. However, for the helium diluted films, the Urbach energy increases with increase in helium dilution indicating the degradation of film properties with increasing the helium dilution of silane in HW-CVD. From the present study it has been concluded that

@ 2013 NSP
Natural Sciences Publishing Cor.

the addition of hydrogen and argon with silane in HW-CVD has beneficial effect on improvement of nc-Si:H film properties and addition of helium has an adverse effect on them.

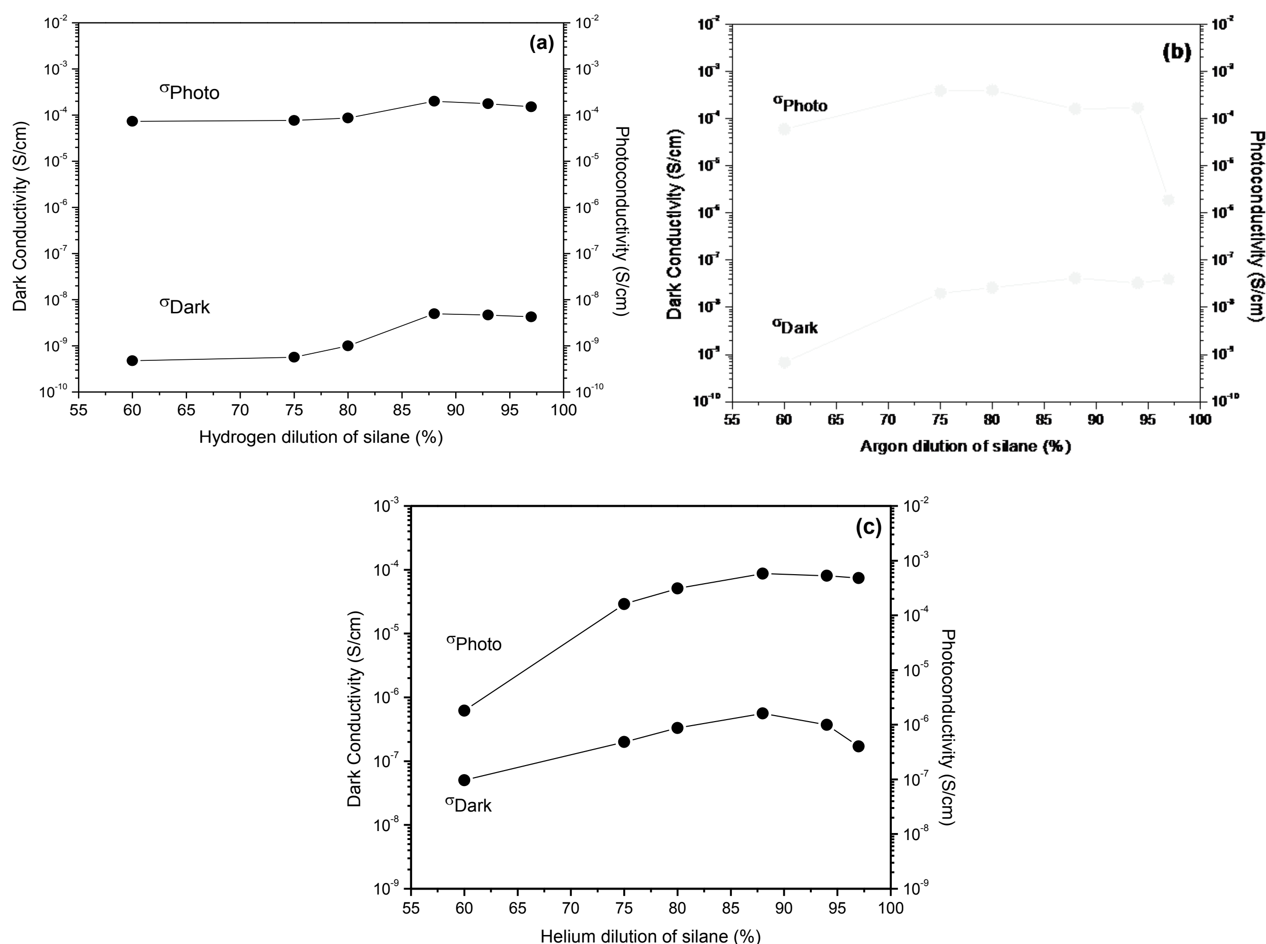


**Figure 6:** Variation of dark and photoconductivity as a function of dilution of silane using different diluents for the nc-Si:H deposited thin films by HW-CVD.

## References


[1] P. Kumar, F. Zhu, A. Madan, "Electrical and structural properties of nano-crystalline silicon intrinsic layers for nano-crystalline silicon solar cells prepared by very high frequency plasma chemical vapor deposition", *Int. J. of Hydrogen Energy* **33**, 3938-3944 (2008).

[2] M. Donker, B. Rech, F. Finger, W. Kessels, M. Sanden, "Highly efficient microcrystalline silicon solar cells deposited from a pure SiH4 flow", *Appl. Phys. Lett*. **87**, 263503-263505 (2005).

[3] Y. Nasuno, M. Kondo, A. Matsuda, "Key Issue for the Fabrication of High-Efficiency Microcrystalline Silicon Thin-Film Solar Cells at Low Temperatures", *Jpn. J. Appl. Phys*. **41**, 5912-5918 (2002).

[4] A. Shah, J. Meier, E. Sauvain, C. Droz, U. Kroll, J. Guillet, U. Graf, "Microcrystalline silicon and 'micromorph' tandem solar cells", *Thin Solid Films* **403-404**, 179-187 (2002).

[5] H. Hsiao, H. Hwang, A. Yang, L. Chen, T. Yew, "Study on Low Temperature Facetting Growth of Polycrystalline Silicon Thin Films by ECR-CVD Downstream Plasma with Different Hydrogen Dilution", *Appl. Surf. Sci.* **142**, 316-321 (1999).


@ 2013 NSP
Natural Sciences Publishing Cor.

[6] R. Saleh, N. H. Nickel, "Raman spectroscopy of B-doped microcrystalline silicon films", *Thin Solid Films* **427**, 266-269 (2003).

[7] H. Weisman, A. Ghosh, T. McMahon, M. Strongin, "a- Si:H produced by high- temperature thermal decomposition of silane*", J. Appl. Phys*. **50**, 3752-3755 (1979).

[8] H. Matsumura, "Study on catalytic chemical vapor deposition method to prepare hydrogenated amorphous silicon", *J. Appl. Phys.* **65**, 4396-4402 (1989).

[9] J. Doyle, R. Robertson, G. Lin, M. He, A. Gallagher, "Production of high- quality amorphous silicon films by evaporative silane surface decomposition", *J. Appl. Phys.* **64**, 3215-3223 (1988).

[10] P. Brogueira, J. Conde, S. Arekat, V. Chu, "Amorphous and microcrystalline silicon films deposited by hot- wire chemical vapor deposition at filament temperatures between 1500 and 1900 °C", *J. Appl. Phys.* **79**, 8748-8760 (1996).

[11] M. Scriba, D. Britton, C. Arendse, M. Staden, M. Härting, "Composition and crystallinity of silicon nanoparticles synthesised by hot wire thermal catalytic pyrolysis at different pressures", *Thin Solid Films* **517/12**, 3484-3487 (2009).

[12] S. Jadkar, J. Sali, S. Kshirsagar, M. Takwale, "The effect of substrate temperature on HW-CVD

[13] deposited a-SiGe:H films", *J. Non-Cryst. Solids* **299-302**, 168-173 (2002).

[14] M. Konagai, " Deposition of new microcrystalline materials, μc-SiC, μc-GeC by HWCVD and solar cell applications", *Thin Solid Films* **516/5**, 490-495 (2008).

[15] H. Matsumura, "Catalytic Chemical Vapor Deposition (CTC–CVD) Method Producing High Quality Hydrogenated Amorphous Silicon", Jpn*. J. Appl. Phys.* **25**, L949-L951 (1986).

[16] A. Mahan, J. Carapella, B. Nelson, R. Crandall, I. Balberg, "Deposition of device quality, low H content amorphous silicon", *J. Appl. Phys.* **69**, 6728-6730 (1991).

[17] A. H. Mahan, "An update on silicon deposition performed by hot wire CVD", *Thin Solid Films* **501**, 3-7 (2006).

[18] C. Horbach, W. Beyer, H. Wagner, "Investigation of the precursors of a-Si:H films produced by decomposition of silane on hot tungsten surfaces", *J. Non-Cryst. Solids* **137-138** 661-664 (1991).

[19] A. Morral, J. Bertomeu, P. Cabarrocas, "The role of hydrogen in the formation of microcrystalline silicon", *Mater. Sci. Eng.:B* **69-70**, 559-563 (2000).

[20] S. Sriraman, S. Agarwal, E. Aydil, D. Maroudas, "Mechanism of hydrogen-induced crystallization of amorphous silicon", *Nature* **418**, 62-65 (2002).

[21] S. Sriraman, M. S. Valipa, E. S. Aydil, D. Maroudas, "Hydrogen-induced crystallization of amorphous silicon thin films. I. Simulation and analysis of film postgrowth treatment with H2 plasmas", *J. Appl. Phys.* **100**, 053514 (2006).

[22] J. Gu, M. Zhu, L. Wang, F. Liu, B. Zhou, Y. Zhou, G. Li, "The compact microcrystalline Si thin film with structure uniformity in the growth direction by hydrogen dilution profile", *J. Appl. Phys*. **98**, 093505 (2005).

[23] R. Schropp, J. Rath, H. Li, "Growth mechanism of nanocrystalline silicon at the phase transition and its application in thin film solar cells", *J. Cryst. Growth* **311**, 760-764 (2009).

[24] N.A. Bakr, A.M. Funde, V.S. Waman, M.M. Kamble, R.R. Hawaldar, D.P. Amalnerkar, V.G. Sathe, S.W. Gosavi, S.R. Jadkar, "Role of argon in hot wire chemical vapor deposition of hydrogenated nanocrystalline silicon thin films", *Thin Solid Films* **519**, 3501–3508 (2011).

[25] S. Jadkar, J. Sali, M. Takwale, D. Musale, S. Kshirsagar, "Synthesis of highly conductive boron-doped p-type hydrogenated microcrystalline silicon (μc-Si:H) by a hot-wire chemical vapor deposition (HWCVD) technique", *Sol Energy Mater Sol Cells* **64**, 333-346 (2000).

[26] M. Brodsky, M. Cardona, J. J. Cuomo, "Infrared and Raman spectra of the silicon-hydrogen bonds in amorphous silicon prepared by glow discharge and sputtering", Physical Review B **16**, 3556-3571 (1977).

[27] J. Tauc, "Optical Properties of Solids", North Holland, Amsterdam (1972).

[28] D. W. Marquardt, " An algorithm for least-squares estimation of non-linear parameters", *J. Soc. Ind. Appl. Math*. **11/2**, 431-441 (1963).

[29] T. Kaneko, M. Wakagi, K. Onisawa, T. Minemura, "Change in crystalline morphologies of polycrystalline silicon films prepared by radio- frequency plasma- enhanced chemical vapor deposition using SiF4+H2 gas mixture at 350 °C", *Appl. Phys. Lett*. **64**, 1865-1867 (1994).

[30] Y. He, C. Yin, G. Cheng, L. Wang, X. Liu, G. Y. Hu, "The structure and properties of nanosize crystalline silicon films", *J. Appl. Phys*. **75**, 797-803 (1994).

[31] Fritzsche, M. Tanielian, C. Tsai, P. Gaczi, "Hydrogen content and density of plasma- deposited amorphous silicon- hydrogen", *J. Appl. Phys* **50**, 3366-3369 (1979).

[32] C. Tsai, R. Thompson, C. Donald, F. Ponce, G. Anderson, B. Wacker, "Transition from Amorphous to Crystalline Silicon: Effect of Hydrogen on Film Growth", Material Research Society Symposium Proceedings **118**, 49-54 (1988).

@ 2013 NSP
Natural Sciences Publishing Cor.

[33] A. Middya, S. Hazra, S. Ray, “Growth of device quality amorphous SiGe:H alloys with high deposition rate under helium dilution”, *J. Appl. Phys.* **76**, 7578-7582 (1994).

[34] H. Shanks, C. Fang, M. Cardona, F. Demond, S. Kalbitzer, “Infrared Spectrum and Structure of Hydrogenated Amorphous Silicon”, *Phys. Status Solidi B* ***100***, 43-56 (1980).

[35] H. Richter, Z. Wang, L. Ley, “The one phonon Raman spectrum in microcrystalline silicon”, *Solid State Commun*. **39**, 625-629 (1981).

[36] T. Hikmott, “Interaction of Atomic Hydrogen with Glass”, *J. Appl. Phys.* **31**, 128-136 (1960).

[37] I. Langmuir, G. Mackay, “THE DISSOCIATION OF HYDROGEN INTO ATOMS. Part I. Experimental”, *J. Am. Chem. Soc.* **36** 1708-1722 (1914).

[38] S. Kim, K. Park, J. Jang, “Effect of H2 dilution on the growth of low temperature as- deposited poly- Si films using SiF4/SiH4/H2 plasma”, *J. Appl. Phys.* **77**, 5115-5118 (1995).

[39] D. Milovzorov, T. Inokuma, Y. Kurata, S. Hasegawa, “Relationship Between Structural and Optical Properties in Polycrystalline Silicon Films Prepared at Low Temperature by Plasma- Enhanced Chemical Vapor Deposition”, *J. Electrochem. Soc.* **145**, 3615-3620 (1998).

[40] M. Jana, D. Das, A. Barua, “Role of hydrogen in controlling the growth of μc-Si:Hfilms from argon diluted SiH4 plasma”, *J. Appl. Phys*. **91**, 5442-5448 (2002).

[41] D. Raha, D. Das, “Hydrogen induced promotion of nanocrystallization from He-diluted SiH4 plasma”, *J. Phys. D: Appl. Phys.* **41**, 085303 (2008).

[42] K. Bhattacharya, D. Das, “Effect of deposition temperature on the growth of nanocrystalline silicon network from helium diluted silane plasma”, *J. Phys. D: Appl. Phys.* **41**, 155420 (2008).

[43] S. Wagner, S. Wolf, J. Gibson, “The Role of Hydrogen in Silicon Microcrystallization”, *Mater. Res. Soc. Symp. Proc.* **164**, 161-170 (1989).

[44] A. Shah, J. Meier, E. Sauvain, N. Wyrsch, C. Droz, U. Graf, “Material and solar cell research in microcrystalline silicon”, *Sol Energy Mater Sol Cells* **78**, 469-491 (2003).

[45] A. Jones, W. Ahmed, I. Hassan, C. Rego, H. Sein, M. Amar, M. Jackson, “The impact of inert gases on the structure, properties and growth of nanocrystalline diamond”, *Journal of Physics : Condensed Matter* **15**, S2969-S2975 (2003).

[46] H. Shanks, C.Fang, M. Cardona, F. Demond, S. Kalbitzer, “Infrared Spectrum and Structure of Hydrogenated Amorphous Silicon”, *Phys. Status Solidi B* **100**, 43-56 (1980).

[47] W. S. Lau, “Infrared characterization of microelectronics”, World Scientific, Singapore (1999).

[48] T. Itoh, K. Yamamoto, H. Harada, N. Yamana, N. Yoshida, H. Inouchi, S. Nonomura, S. Nitta, “Role of hydrogen in hydrogenated microcrystalline silicon”, *Sol Energy Mater Sol Cells* **66**, 239-244 (2001).

[49] C. Arendse, G. Malgas, T. Muller, D. Motaung, S. Halindintwali, B. Mwakikunga, “Thermally Induced Nano-Structural and Optical Changes of nc-Si:H Deposited by Hot-Wire CVD”, *Nanoscale Research Letters* **4**, 307-312 (2009).

[50] J. Baugh, D. Han, K. Kleinhammes, Y. Wu, “Magnetic susceptibility and microstructure of hydrogenated amorphous silicon measured by nuclear magnetic resonance on a single thin film”, *Appl. Phys. Lett*. **78**, 466-468 (2001).

[51] G. Cody, C. Wronski, B. Abeles, R. Stephens, B. Brooks, “Optical characterization of amorphous silicon hydride films”, *Solar cells* **2**, 227-243 (1980).

[52] J. Tauc, R. Grigorovici , A. Vancu, “Optical Properties and Electronic Structure of Amorphous Germanium”, *Phys. Status Solidi* **15**, 627-637 (1966).

[53] G. D. Cody, “Disorder and the Optical-Absorption Edge of Hydrogenated Amorphous Silicon”, *Phys. Rev. Lett.* **47**, 1480-1483 (1981).

[54] C. Rotaru, S. Nastase, N. Tomozeiu, “Amorphous Phase Influence on the Optical Bandgap of Polysilicon”, *Phys. Status Solidi A* **171**, 365-370 (1999).

[55] D. Beeman, R. Tsu, M. Thorpe, “Structural information from the Raman spectrum of amorphous silicon”, *Phys. Rev. B* **32**, 874-878 (1985).

[56] T. Saitoh, T. Shimada, M. Migitaka, “Preparation and properties of microcrystalline silicon films using photochemical vapor deposition”, *J. Non-Cryst. Solids* **59-60**, 715-718 (1983).

[57] S. Saha, A. Barua, S. Ray, “The role of hydrogen dilution and radio frequency power in the formation of microcrystallinity of n- type Si:H thin film”, *J. Appl. Phys.* **74**, 5561-5568 (1993).

@ 2013 NSP
Natural Sciences Publishing Cor.